■ Scientific Justification

1.1 Introduction

Hubble Space Telescope (HST) is universally regarded as one of the most successful science missions in history. We have designed a Multi-Cycle Treasury (MCT) program that targets outstanding questions in extragalactic astronomy and cosmology while delivering data products of immense value to the community, particularly in planning programs with upcoming facilities such as the James Webb Space Telescope (JCMT), the Atacama Large Millimeter Array (ALMA) and the next generation of extremely large ground-based telescopes (ELTs) and missions designed to probe dark energy. Our program exploits HST's unique role: *superlative angular resolution* and, via the newly-installed Wide Field Camera 3 (WFC3/IR), a *deep imaging capability* that exploits the *low infrared background* of space. Building on a considerable legacy of deep ACS imaging in two fields comprehensively studied by the various Great Observatories, our program is motivated by three outstanding scientific questions.

(i) The First Galaxies: When did the first galaxies assemble and is their collective ultraviolet (UV) radiation sufficient to reionize the Universe at early times? The period corresponding to the redshift range $7< z <10$ is now the frontier in our understanding of galactic history. Upcoming facilities are poised to study individual distant sources to verify their redshift and emission line properties as well as ultimately to reveal their composition and baryonic content as proof they may contain pristene first-generation stars. Early work within the Ultradeep Field (UDF) has shown the promise of HST in this area and our team has swiftly marshaled resources to analyze these data. We now propose to substantially augment the available data in both GOODS fields to address the nature and role of early galaxies in cosmic reionization. Our resulting sample will provide targets for immediate study and lead to optimized observational strategies with future facilities.

(ii) The Nature of Dark Energy: The accelerating Universe points to a fundamental mystery in the physical sciences: does the vacuum of space have an unforeseen energy density, and is this a constant property or the manefestation of a time-varying scalar field? Or is this 'dark energy' an illusion that hides a more profound discovery to be made about the Universe? HST is uniquely positioned to make progress by securing the first measure of the expansion history based on Type Ia supernovae (SNe Ia) to redshifts $z \simeq 2.5$. This will provide a clear test of whether current hypotheses for dark energy are correct. Using our team's experience with the successful Supernova Legacy Survey(SNLS), we propose a rolling search which, augmented with a targeted ToO campaign, will provide the definitive body of SNe Ia data over $0< z < 2.5$ for the next decade. This large leverage in redshift will be a necessary precursor in ensuring a valid role for SNe Ia with future facilities such as the Joint Dark Energy Mission (JDEM).

(iii) The Emergence of the Hubble Sequence: Our understanding of the growth of structure is best on *large scales* where the interplay of gravity and matter is simple. On the scale of galaxies, our understanding of the range of masses, sizes and luminosities is based only on the imagined interplay between the collapse of dark matter halos, the formation of stars

and black holes, and the non-gravitational feedback from related energy sources. Earlier HST data has shown that massive spheroidals and disk galaxies appear at redshifts 1-2. But by what processes do these galaxies develop the finer details of morphological structure (bulges, bars, spiral arms) essential for a full understanding of the history of the Hubble sequence - an outstanding goal for which HST was purposely designed? Ground-based telescopes with adaptive optics (AO) can now fully exploit HST's unique imaging capability by studying the internal dynamics and other properties of representative sources. We propose to augment the GOODS ACS dataset with appropriately deep WFC3 imaging, stacked from many independent visits, producing a database of finely-sampled images of the assembling stellar mass for a variety of synergistic programs concerned with tracking the emerging Hubble Sequence.

The two GOODS fields are chosen for this MCT program because they contain the largest repository of Great Observatories data with, for the foreseeble future, the deepest optical to mid-infrared imaging. Two fields ensures access from both hemispheres and mitigates cosmic variance. The GOODS field sizes are also well-matched to extant ground-based optical and near-infrared spectrographs. Embarking on an effort to go deep in new fields make no strategic sense in the final years of the Great Observatory program. While a case can always be made for studying larger areas, as a narrow field instrument we believe HST is not efficiently employed undertaking shallow exposures over panoramic areas. In its final years HST should concentrate on what it can do best: providing exquisitely deep data of high angular resolution in order to establish the foundation for future facilities.

We develop the detailed science case for each of these areas in the sub-sections below. Each leads to science requirements in terms of depth, filter coverage and survey area which we merge into an observational strategy in §3.

1.2 The First Galaxies:

Locating and characterizing the earliest known galaxies represents the final frontier in constructing the story of cosmic evolution. Measuring the abundance and luminosity distribution of $7 < z < 10$ galaxies will determine whether or not the Universe was reionized by UV photons from star-forming galaxies. Such data will also provide vital constraints on early 'feedback' mechanisms which inhibit growth in primordial systems and govern the subsequent evolution of dwarf galaxies seen around present-day galaxies. Progress has largely been enabled via deep multi-color ACS imaging of the GOODS and UDF fields. Hundreds of faint galaxies to $m_{AB} \simeq 27$, selected using the Lyman break technique (LBGs) have now been confirmed spectroscopically over $4 < z < 6$ with ground-based telescopes [St10]. Ultra-deep IRAC photometry has provided stellar masses and luminosity-weighted ages [St09]. These studies reveal a declining abundance of star-forming galaxies over $3 < z < 7$, raising doubts that the UV output of luminous galaxies can sustain reionization as required by measures of electron scattering in the microwave background [Bu09, McL09b,Oe09]. However, as the stellar mass density at $z \simeq 5$–6 is significant [St09], attention is now focused on lower luminosity galaxies at $z \simeq 7$–8. If these are abundant and perhaps host metal poor stellar populations, they could dominate the UV luminosity density at early times. This year we secured improved ground- and HST-based data beyond $z \simeq 7$. We used deep Subaru imaging to $Y_{AB} \simeq 26$ over 0.5 degree^2 to reveal $\simeq 10$ z'-drop galaxies constraining the bright end of UV luminosity function (LF, Ou09) and ultra-deep WFC3/IR imaging of the UDF has complemented this with constraints on the faint end, as well as a first estimate of the comoving number density at $z \simeq 8$ (Fig. 1a; McL09, B09).

HST is pivotal to further progress. The depth attained with WFC3/IR in the UDF ($Y_{105}, J_{125}, H_{160} \simeq 29$(AB)) is impressive. The use of 3 IR filters is advantageous in reducing foreground contamination [McL09b] and in measuring the rest-frame UV continuum slope - a key diagnostic of evolution in the stellar populations [Bou09]. Future ground-based imaging surveys (Subaru HSC, UltraVISTA) will not even reach m_{AB} $\simeq$27.5, i.e. a $L^\star$ galaxies at z $\simeq$7. The current WFC3/IR survey (GO 11563; PI: Illingworth) addresses only a small survey area ($\simeq$ 12 arcmin^2 upon completion), resulting in $\simeq$ 40% cosmic variance uncertainties at $Y_{105} = 28$.

Our proposed MCT program will revolutionize our understanding of the Universe at $z > 7$, and prepare the community for optimal use of JWST. We have carefully designed our program to fully exploit both the unique power of WFC3/IR, and the existing investment in deep *HST*-ACS and *Spitzer*-IRAC imaging. A crucial feature is the use of parallel ACS observations to push z_{850} ACS imaging to the depth required for full exploitation of the WFC3/IR data. This transformational survey will enable us to address the following key questions:

• What is the form of the LF and total UV luminosity density at z$\simeq$7 (Fig. 1)? Our survey will reach $\simeq$ 1.5 magnitudes below L^* via an enlarged sample of $\simeq$400 galaxies spanning $-18.7 < M_{1500} < -21.0$. By observing two well-separated $\simeq$ 100 arcmin^2 fields, cosmic variance uncertainties (at $\simeq L^*$) will be reduced from $\simeq$ 40% to $\simeq$ 15%, allowing the first robust comparison with theory.
• Is the abundance of star-forming galaxies at z $\simeq$8–9 consistent with the deductions made above? The current HST survey will yield only a handful of possible candidates. We will increase this number 20-fold to $\simeq$ 150 galaxies. Sampling the LF down to $M_{1500} \simeq -18.7$ will enable us to perform the first proper fit to the $z \simeq 8$ LF for insertion into re-ionization calculations as well as securing the first glimpse of the z $\simeq$9–10 population.
• What is the physical nature of early galaxies, particularly the abundant low luminosity examples? Further enhanced by the Spitzer-warm Extended Deep Survey (SEDS) observations, the IRAC data in GOODS will remain the deepest ($m_{3.6} \simeq 28$, 2σ). This will enable individual detections for the brighter $z \simeq 8$ galaxies and statistical measurements of stellar masses for fainter galaxies reaching to $J_{125} = 28.3$ (5σ). We will thus, for the first time, be able to determine how HST sizes and UV continuum slopes of representative $z = 7 - 9$ galaxies depend on luminosity, age/metallicity and stellar mass.

The above will clearly provide an important treasury for immediate and future spectroscopic campaigns. We expect >500 galaxy candidates with $z > 6.5$ over 200 arcmin^2 ensuring an adequate surface density for deep multi-object spectroscopic campaigns. Our team has led the field in confirming ACS-selected LBGs with $4 < z < 7$ and is poised, via this proposal, to undertake equivalent campaigns for z $\simeq$7–8 sources with infrared spectrographs to which our international team has privileged access. Prior to JWST, an important target is to confirm the possible decrease in the fraction of Lyα emitting galaxies due to attenuation that might be induced by an increased abundance of neutral hydrogen (c.f. Ou09). We estimate that ambitious, but practical, multi-night exposures with Keck/MOSFIRE and VLT/KMOS would detect Lyα emission (5σ) with 20Å rest-frame equivalent widths to $J_{125} \simeq 28$ thereby confirming or otherwise the extent to which the intergalactic medium remains ionized to $z \simeq 8$ (Fig. 2a). NIRSpec on JWST will yield R=100 spectra vital for confirming steep UV continuum slopes and detailing the degree of nebular contamination of broad-band spectral energy distributions (Fig. 2b). This capability extends to the flux limit of our proposed survey at $J_{AB} \simeq 28$, with NIRSpec integration times $\simeq 5 \times 10^4$ secs. **Incomplete - need Andy's figure etc**

1.3 The Nature of Dark Energy

Supernovae (SNe) of all types provide valuable insight into the physical processes driving the evolution of matter and energy in the Universe. Those of Type Ia (SN Ia) provide the most direct evidence for cosmic acceleration and the proposed "dark energy" that drives it. The unresolved nature of SNe within their host galaxies plus the requirement for well-calibrated light curves means that *HST* has played an unique role in extending the Hubble diagram of SNe Ia beyond redshift one (Ri04,07).

A large redshift lever arm for studying SNe Ia is desirable for many reasons. Foremost, so little is known about the theoretical basis of dark energy that any observational constraints on the early expansion history are vital input. Although data currently suggest the equation of state for vacuum energy – $w = p/\rho$ – has w=-1.0 to within ∼7% as required by a cosmological constant (e.g. Ke09), the data permit a variety of exotic time-varying possibilities, as well as cosmologies where the expansion history is not governed by standard General Relativity (Rub09; Sol09). Improving the Hubble diagram beyond $z \simeq 1$ via a *HST* campaign offers the most likely route to detecting departures from a cosmological constant and thus an option for a breakthrough (Fig. 3).

Secondly, the study of SNe Ia seen when the Universe was only 3–4 Gyr old will provide new insights into the physics of SN Ia explosions and their role in the chemical enrichment. Recent studies have linked the rate of SNe Ia with the star formation properties of their host galaxies (Man05, Sull06, Aub09). As the abundance of star-forming galaxies was significantly higher at large redshift, the rate of SNe Ia should consequently be larger. As SNe Ia are the primary source of iron, a significant population of SNe Ia at high-redshift has implications for the enrichment history in galaxy formation models.

Much progress has been realized in the study of distant SNe Ia since the early campaigns that discovered dark energy. The SNLS demonstrated the utility of a "rolling search" in four 1 deg^2 fields leading to uniform quality multicolor light curves. ACS was used during Cycles 11-13 within the GOODS fields to locate ∼15 spectroscopically-confirmed and cosmologically useful SNe Ia over $1 < z < 1.6$. The latter campaign relied on F850LP detections and grism spectroscopy – but poor light curves prevented a robust parameterization of luminosities and colors. Although this data hints at a decelerating period (Fig. 3), the uncertainties are considerable, as evidenced by tension in the distances derived by different groups. Some find these events brighter than expected in ΛCDM (Kow08) and others fainter (Kess09); the net effect is that SN Ia constraints at $z > 1$ remain poor.

By breaking our deep WFC3/IR survey (§1.2) into a number of discrete visits, we propose a 'rolling search' in J_{125}, generating a similar number of SNe Ia as in the earlier ACS campaign but at higher redshift. Via the strategy and associated simulations discussed in §3, and in conjunction with existing ACS and ground-based $z < 1$ data, we can address the following key questions:

• *Did the Universe witness a decelerating phase beyond a redshift 1?* By extending the Hubble Diagram to $z > 2$ with increased precision, an exciting possibility is the detection of departures from a cosmological constant (Fig. 3). Most existing studies of dark energy are, perhaps naturally, driven by "figure of merit" considerations, aimed either at tightening constraints on the time-averaged value of w, or on simplistic models of its variation with redshift. Our HST campaign tests a more fundamental question compared to incremental improvements in parameter estimation: Does dark energy behave like a cosmological constant at early times? *Any* SN Ia observations discrepant with the cosmological constant would short-cut a decade of ground-based observational effort. By probing a redshift range that otherwise will only be accessible when, or if, dedicated missions become available, *HST* has a unique opportunity to pre-empt these missions in the next 2 years.

Dark energy physics can provide a multitude of possibilities to explain the cosmic acceleration (e.g. Cop06). Each can be made consistent with low-z SN Ia data but their predictions differ at higher-z (Fig. 3). Options include dynamical scalar fields, modified gravity arising from extra dimensions, Chaplygin gases which attempt to unify dark energy and dark matter and kinematic parametrizations of the acceleration. Further explanations postulate potential biases in the SN Ia method, such as evolution or grey dust – again, high-z SNe can test these possibilities.

• *What is the delay-time of a SN Ia explosion?* Fig. 4 demonstrates how different progenitor models predict different numbers of SNe Ia at $z > 1.5$. Current data suggest a short average delay-time (see discussion in §3), but previous *HST* surveys found a lower than expected rate at $z \sim 1.5$ (Dah08). This was interpreted as evidence for a $\simeq$3Gyr delay-time. However, these HST searches were conducted in the rest-frame UV where the dispersion in SN Ia properties is large (E08) and extinction plays a significant role. A search conducted in a redder observer-frame filter, such as J_{125}, will not be susceptible to these biases until $z > 2.5$ and will resolve these outstanding issues.

Each SN Ia will have a partial J_{125} light curve from the rolling search, which we will supplement with additional Y_{105} and H_{160} ToO observations (see §3,4). As for the earlier ACS search, we aim to secure $\sim$15 events but at higher redshift leading to constraints shown in Fig. 3.

A spectroscopic redshift would allow robust photometric typing of the SN light curves. We will observe all likely candidates with a concerted ground-based campaign prior to triggering a ToO using additional Keck, VLT and Gemini spectroscopic campaigns. Even if no robust SN type is forthcoming, these observations will eliminate lower-z interlopers, and will yield a host galaxy spectroscopic redshift, in addition to photometric redshifts based on the rich GOODS database.

Faint transients other than SNe Ia will be found in the survey. There is a huge potential for fundamental new discoveries, for example in very distant luminous hyper-events, SNe IIP's and II-N's as highlighted in our recent SNLS and Palomar Transient Factory (PTF) discoveries [Nugent07, Q09, Cook09]. As discussed in §7, we will promptly. publicize all discovered transients.

1.4 Emergence of the Hubble Sequence

Whereas panoramic ACS imaging has revealed morphological and size information at high redshift, the physical details necessary to understand how the Hubble sequence forms will only come from studies of the detailed *internal stellar mass structures* of distant galaxies. *Superlative depth*, unique to HST, is required to detect these internal structures and *the full PSF resolution of HST* is required to resolve them. The Hubble Sequence assembles by $z \sim 1$ through complex interplay between secular processes, mergers and feedback - from star formation and active galactic nuclei. Theoretical models have made great progress, but discrepancies with observations remain: massive galaxies appear to form before less luminous objects objects, the role of mergers is not observationally well-determined and secular processes such as bar instabilities and gas starvation may play a role in shaping morphologies. And although AGN feeback likely plays a central role through the co-evolution of black holes and galaxies, this well-discussed hypothesis is still not empirically corroborated.

Deep, multi-band, and high angular resolution *near infrared imaging* is essential for progress. Only by measuring the stellar mass of subgalactic components beyond $z \sim 1$ can we directly reconstruct the diverse and complex modes of galaxy assembly. Our survey will address some of the most compelling outstanding issues in galaxy formation as summarized below:

•*From chaos to order; the formation of the Hubble Sequence* $1 < z < 2.5$*:* Massive galaxies with z <1 typically have smooth stellar components and well-ordered kinematics Yet surprisingly, the picture appears to be very different only 2.5 Gyr earlier at $z \simeq 2$, where vigorous star-formation activity occurs almost exclusively in clumpy mass distributions (E09, G08). This transition could indicate a different mode of star formation, perhaps arising from cold streams of dense gas (Keres09, Dek09). Alternatively, resolved kinematic observations argue that smooth star-forming disks at $z \simeq 2$ are easily understood as scaled-up versions of local galaxies (Jones09). Given the diversity of star formation modes and uncertainties in dust correction and M/L we currently do not know how stellar mass is assembled. To make progress in this area we will first determine projected stellar mass density from stellar population synthesis fitting and of SEDs in individual pixels. This information will be used to construct the first stellar mass function segregated by morphological types in the range $z = 1 - 2.5$ (unbiased by morphological k-correction). At a finer level, we will fit models to stellar mass maps to determine the stellar mass function of bulges, disks, bars in the same redshift range. This will enable direct comparison with local studies and will be a new test of semi-analytic models of galaxies formation, and the connection between merger history and morphology (Be07). As shown in Figs. 5 and 6 our proposed images will be sufficient deep and finely-resolved to identify and galactic substructures as small as the bulge and the LMC in this redshift interval. Within both GOODS fields to a realistic selection limit of

$H_{160} \simeq 27$, we expect 17000 galaxies between $1< z <2.5$

How important are mergers for assembling the stellar mass of galaxies as well as triggering ULIRG-like star formation and AGN activity at $z \simeq 2$? Beyond $z \simeq 1$, the merger rate is poorly known because strong K-corrections can mimic the irregular morphologies associated with mergers [Con08] and optical pair counts do not reflect the mass ratios of merging pairs. NICMOS studies of the highest mass galaxies in the UDF suggest a high pair fraction [Blu09] that is at odds with theoretical predictions [Gen08]. The deeper near-IR data proposed will help resolve the importance of mergers at $z \simeq 2$ by providing mass-limited samples of 50–100 major pairs that can be studied as a function of mass and redshift. At lower redshifts, important progress has been possible [Lotz08,Bun09], but this has not been extended to the minor merger regime. Our observations will probe mass ratios of 1:20 for $> 10^{10} M_{\odot}$ galaxies at $z \lesssim 1.5$ (Fig. 6), testing predictions that minor mergers assemble much as 40% of the mass density of local spheroids [Hop09e]. Furthermore, multicolor information will allow us to probe if mergers are associated with star formation or not.

• *The formation of red sequence ellipticals:* The emergence of these systems represents an important landmark in galaxy evolution, indicative of scaling relations that define the Hubble Sequence [Som08]. The very existence of massive red ellipticals found by NICMOS out to $z \sim 2.5$ is currently unexplained by galaxy formation models [G09]. How abundant are they at higher redshifts? A tantalizing detection was claimed in the UDF (CM04) but confirmation of a population requires wider field data. NICMOS also revealed that the examples at $1.5 < z < 2.5$ appear to be *4-5 times smaller* than similarly massive local counterparts [vD08]. Possible solutions include uniform expansion [Fan08,vdW08], growth of extended wings through accretion of low-density material [Hop09d, Nip09], and biased high-z size estimates due to observational limitations [Hop09e]. Dynamical masses from ground-based spectra is challenging and has so far given contradictory results [vD09,Cap09]. Very deep near-IR data of high angular resolution, made possible by fine resampling enabled via our multi-visit strategy (§1.3,3) will detect both the dense inner core and low surface brightness extended structures greatly clarifying the validity of these explanations. Early WFC3 data showcase the importance of deep IR data [Cas09], although their small sample size (6 objects) prevents definite conclusions. Within both GOODS fields, we can expect to conduct such measures for $\simeq$100–200 early ellipticals.

• *The black hole connection:* The tight relationship between black hole mass and bulge velocity dispersion [Gül09, FF05) is now being extended to high redshift [Peng06, Ben09, Jank09]. Early data suggests that black hole growth predates galaxy formation (Fig. 7), in contrast with the expectations of many theoretical models where they are believed to evolve in lockstep so as to reproduce the tightness of the local relations. However, current $z >1$ data samples only the hosts of the most massive black holes ($\sim 10^9 M_{\odot}$). As the low and high z samples are not well matched in black hole mass, mass-dependent evolution, expected as a result of the downsizing trends seen for both star formation and AGN activity, cannot be tested. Second, as high z velocity dispersions are unfeasible, reliance is placed on photometric measurements of the host luminosity [Merl09].

Our survey will readily detect the host bulge and the point source flux of type-1 AGN powered by $> 10^7$ $M_\odot$ black holes for z <3 (Fig. 6). The point source fluxes, in combination with followup ground based spectroscopy of the broad lines will be used to determine black hole masses to 0.4 dex accuracy (e.g. McGill et al. 2008). Based on the black hole mass function determined by [GHo07,09] and correcting for evolution to match the density of broad line AGN in COSMOS at the high mass end, we estimate that 120 ± 50 broad line AGN are present in the GOODS fields and measurable with deep ground based spectroscopy (for comparison ~ 300 AGN are detected in X-ray images of the GOODS-ACS fields [Trei04]). Our multi-epoch strategy will allow us to also detect faint variable point sources via difference imaging (e.g. Sar08) missed by conventional multiwavelength detection techniques.

1.5 Summary of Data Products for the Community: The primary data products for the community will be deep ACS z_{850} and WFC3/IR Y_{105}, J_{125} and H_{160} mosaics of each GOODS field, released incrementally as each visit progress and consolidated annually as each field is completed. All detected transients will be announced as they occur and their photometric data released annually. Associated catalogs to limits appropriate for both intermediate and high redshift studies will be matched with GOODS ACS and ground-based K and spectroscopic data. Further details of data products and associated archival tools are discussed in §7.

Programmatic Impact

Progress in resolving the 3 major topics underpinning this proposal will have far-reaching implications for the physical sciences consistent with major themes in NASA's Strategic Plan. The identification and study of a large population of galaxies in the uncharted redshift range $7< z <10$ will finally determine the role of star-forming galaxies in cosmic reionization - a landmark event in cosmic history - and provide an abundant set of targets for diagnostic spectroscopy with JWST. The fraction of luminous galaxies with Lyα emission will indicate the degree of neutrality in the intergalactic medium ahead of ambitious 21cm surveys. Dark energy remains a mystery with no agreed physical basis. HST has an unique opportunity to secure a precision dataset in the next 2 years. The Hubble diagram for SNe Ia over $0< z <2.5$ will demonstrate one of two things: if deceleration is observed it will convincingly show that dark energy is of the form to be addressed in plans for future facilities such as JDEM (and that SNe are valuable tracers). Alternatively it may reveal a major surprise indicative that the expansion history is not understood. Finally, a physical understanding of the rapid emergence of the Hubble sequence of morphologies, enabled by the combination of HST's exquisite resolution and imaging sensitivity, will be the primary legacy of the mission. Synergy with ground-based large telescopes - now equipped with capabilities for resolved infrared spectroscopy - will be strengthened.

The merger of these 3 major themes into a single proposal is made possible by the early investment of multi-color ACS imaging in the GOODS fields, the performance of the WFC3/IR camera and our multi-visit strategy which enables the detection of transient events and combines to provide images of superlative depth and resolution. Accordingly, it is not strategically sensible to remove any one of the 3 science themes. To secure sufficient $z >1.5$ SNe Ia and $z > 7$ galaxies to make progress necessitates a multi-cycle treasury program.

In the event of a *reduced allocation* (e.g. $\simeq$500 orbits), completing one GOODS field would not be strategically useful since, conducted over two cycles this would seriously increase the cosmic variance and marginalize the SN search (introducing a lower cadence that would confuse rising and declining Ia's). Although clearly our main goals would be marginalized by the factor $\simeq$2 smaller sample, we would reconfigure our pointing strategy to survey two smaller rectangular fields in each of GOODS-N/S that optimally match those of ground-based IR spectrographs.

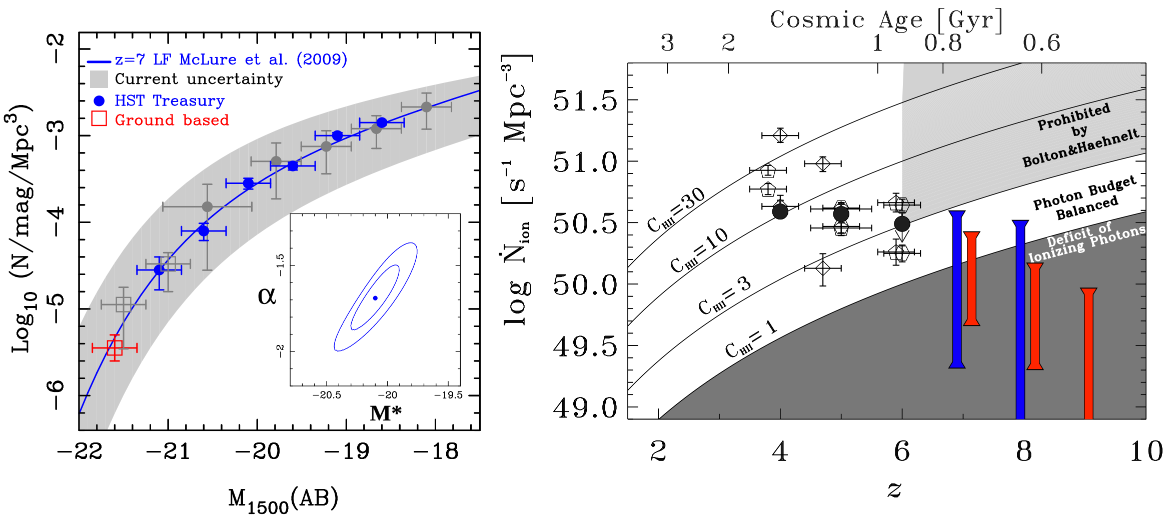

Figure 1: The evolving galaxy UV LF over $7< z <9$ as a new constraint on the physics of reionization. (**Left**) Grey points represent current constraints on the z=7 LF (McL09). Blue points represent the projected LF from the proposed MCT imaging combined with forthcoming ground-based data (UltraVISTA; red points). The inset shows the resulting 1σ & 2σ confidence intervals on α and M*. Equivalent data based for 150 galaxies will be secured at $z \simeq 8$. (**Right**) The rate of ionizing photons per comoving Mpc^3 as a function of redshift. Assuming a photon escape fraction $f_{esc} = 0.2$, solid lines show how the requirements for reionization depend on redshift and clumping factor (Ou09). Measurements at $z < 6$ are indicated by the data points and the blue bars indicate current constraints at $z > 6.5$ (Ou09, McL09b). The red bars illustrate how our new $z > 7$ galaxy samples will provide the first powerful test of reionization physics.

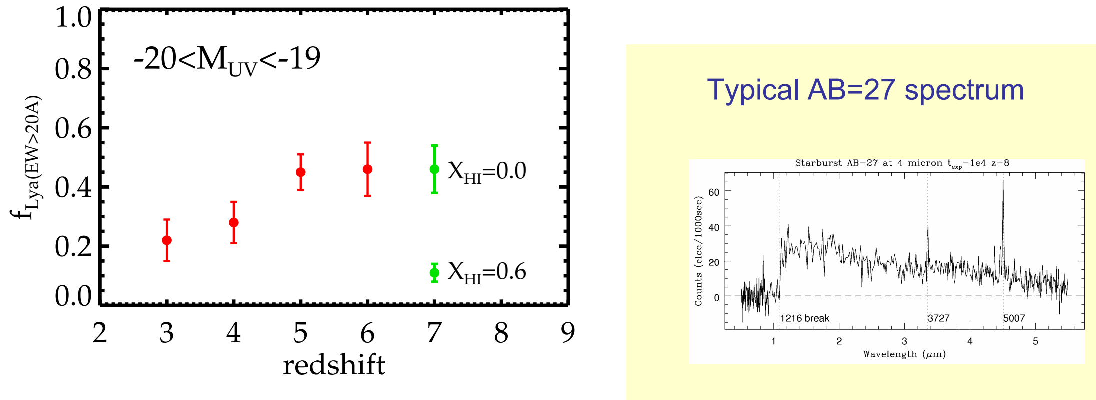

Figure 2: Impact of ground-based and JWST spectroscopic follow-up of $z > 7$, $m_{AB} \simeq 28$ galaxies located in our program. (**Left**) The fraction of galaxies with Lyα emission serves as an additional probe of reionization. Narrowband-selected Lyα emitters at $z \simeq 6-7$ (Ota08,Ou09b) hint at a decrease consistent with an increasing neutral fraction. Ambitious exposures with near-IR multi-object spectrographs on Keck/VLT can detect emission (EW(rest)>20Å) from sources as faint as $J \simeq 28$. Such follow up will distinguish a highly ionized IGM at $z \simeq 7$ (upper green datapoint) from the partially neutral IGM suggested by narrowband studies (lower green datapoint). **Right** Simulated **** sec JWST NIRSPEC spectrum for a $z \simeq 8$, $m_{AB} \simeq 28$ galaxy......

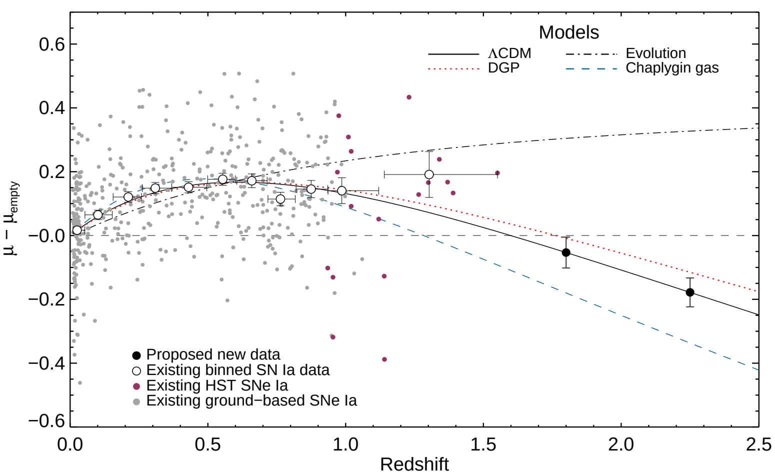

Figure 3: Extending the SN Ia Hubble Diagram beyond z≃: Residual version after subtracting an empty universe model. Grey points represent all current cosmologically-useful SNe; open circles show the data binned in redshift. Filled circles indicate the precision of the proposed data, plotted for simplicity on the ΛCDM prediction. Other lines correspond to plausible models consistent with low-z SN Ia data but which diverge at higher z. These include a DGP model arising from a class of brane-related theories and a Chaplygin gas model that attempts to unify dark energy and dark matter. The dot-dash line shows the trend expected for SN evolution proportional to look-back time.

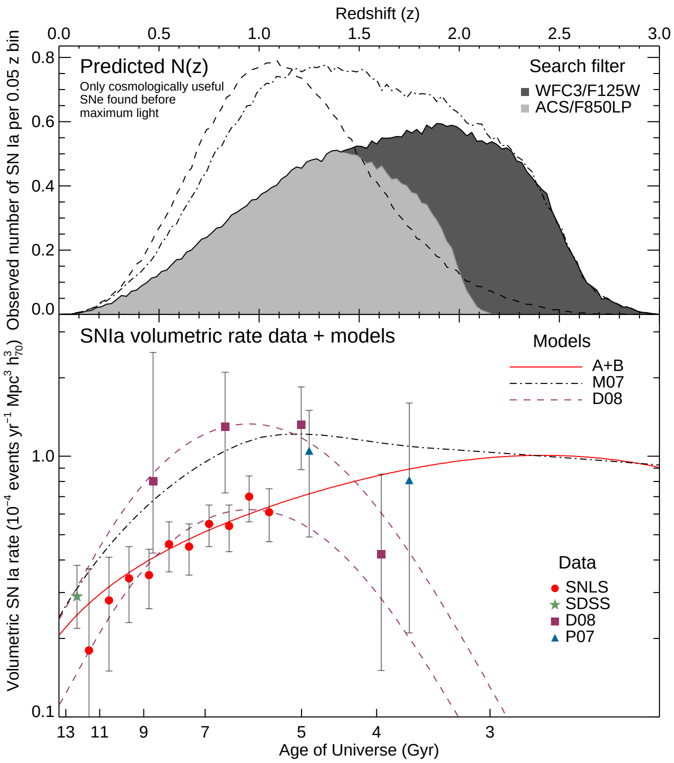

Figure 4: SN Ia rates and expected survey outcome: The volumetric SN Ia rate evolution (lower panel), well-defined by SDSS and SNLS at $z < 1$, is uncertain at $z > 1$. Nonetheless, rate evolution closely tracks the star-formation history: either two-component "A+B" models (solid line; SB05), or the Mannucci et al. delay-time distribution (dot-dash line; Man06,07). Models with a delay-time of $\sim$3 Gyr (dashed line; Dah08) predict fewer z >1.5 SNe but do not fit the lower z data. The original Dah08 model (upper dashed line) does not fit the SNLS data, and a revised version which fits the SNLS data (lower line) misses the SDSS point. The upper panel shows the expected $N(z)$ for our SN search based upon the A+B parameterization.

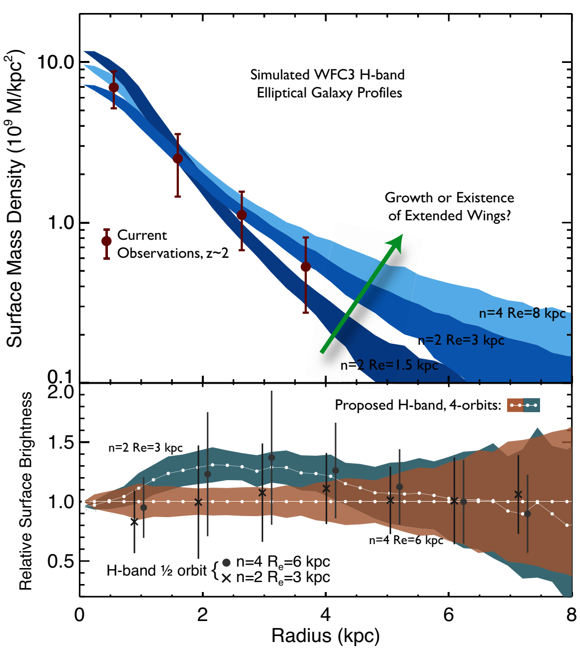

Figure 5: Elliptical galaxy profiles at $z \sim 2$. (**Top:**) Shaded regions trace the mean and 1-σ uncertainties for 3 simulated M_* ellipticals convolved with the PSF, pixel size, and noise of the proposed 4-orbit H_{160} data. NICMOS data (points with error bars) favor compact profiles but cannot detect extended, low-surface brightness wings. The proposed WFC3 images would track the emergence of extended wings with time ($z \lesssim 1.5$) as proposed by [Hop09d]. (**Bottom:**) Relative brightness of two Sersic profiles with R_e=3 and 6 kpc. The proposed dithering strategy easily distinguishes the two (dotted lines with shading) while half-orbit exposures (data points with error bars) cannot.

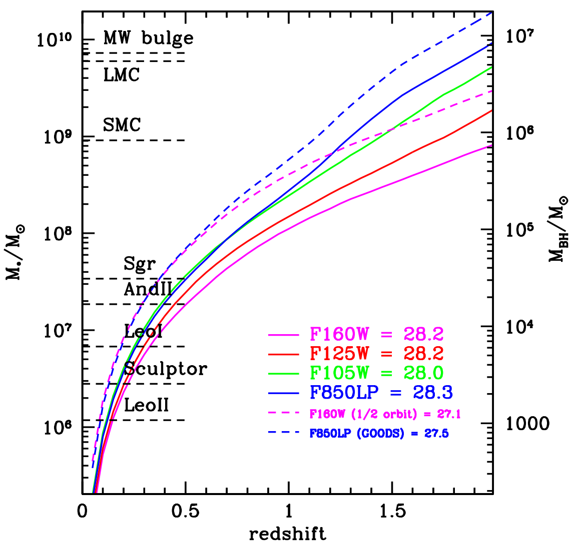

Figure 6: The limiting stellar mass (5-σ) for substructure as revealed for – the present proposal, the existing GOODS z' images and a shallow panoramic HST survey. Galactic sub-structures such as the Milky Way bulge or Magellanic Clouds can be detected to z$\simeq$2 in all bands ensuring accurate stellar mass estimates. The right vertical axis shows the corresponding black hole mass limit assuming a typical luminosity of 10% of their Eddington limit and the standard bolometric correction factor [El94]. At the proposed depth active black holes with masses above 10^7 $M_\odot$ can be detected to beyond $z \simeq 2$.

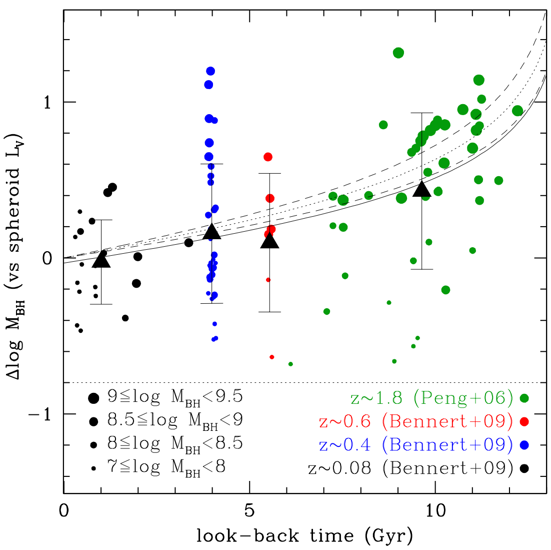

Figure 7: Black hole mass vs host bulge luminosity (passively evolved to $z = 0$). The offset, $\Delta\, M_{BH}$, from the local relation suggests that black hole growth predates bulge growth. However, evolution may be mass dependent due to known downsizing trends. With current data only the most massive black holes can be probed at high redshift. Our proposed observations will allow us to detect *all* type-1 AGN with M_{BH} above 10^7 $M_\odot$ and measure the host bulge *stellar mass*, thus removing the dominant uncertainty of luminosity evolution correction.

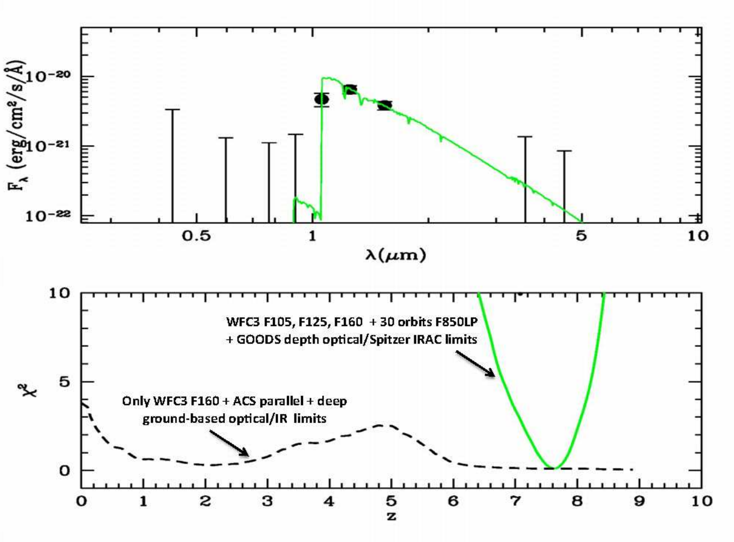

Figure 8: Advantage of our strategy in locating high z objects: SED fits and redshift likelihoods (χ^2, green line) for a $z = 7.6$ galaxy with $H_{160} = 27.8$ and colors similar to a UDF object [McL09]; photometric uncertainties are consistent with the depth of the proposed program; ACS and IRAC limits are consistent with data in the GOODS fields. The dashed black line illustrates the reduced precision for observation in H_{160} only (no Y_{105}, J_{125}) with parallel observations in one ACS filter combined with deep ground-based optical/near-IR upper-limits (e.g. deep Subaru, CFHT, VISTA or Hawk-I imaging). Our WFC3/IR 3-filter strategy with ACS parallels that augment limits only available in the GOODS fields is clearly essential for locating the Lyman-break and measuring the rest-frame UV slope.

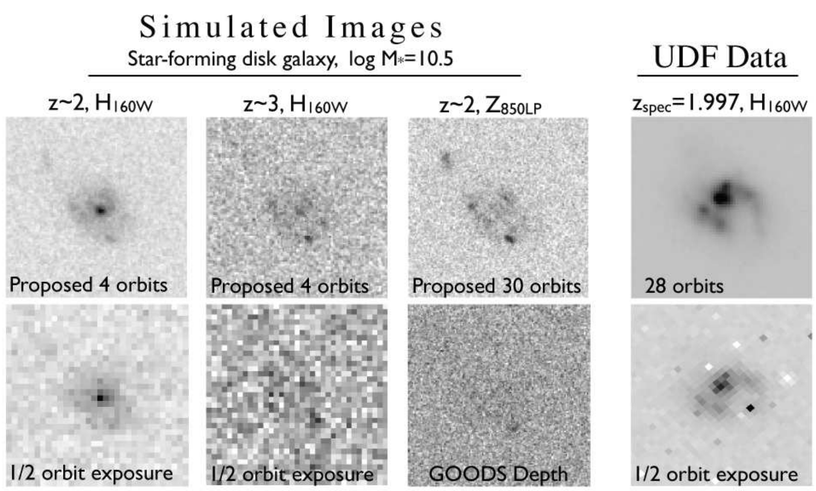

Figure 9: Importance of depth and resolution in probing internal structures: simulated images of a star-forming disk galaxy ($\log M_*/M_\odot \approx 10.5$) redshifted to $z \sim 2$ and 3, as viewed with different filter bands, exposures, and pixel sizes. Sub-components are only detectable via dithered multiple exposures. (Right) UDF H_{160} images of a $z_{spec} = 1.997$ galaxy.

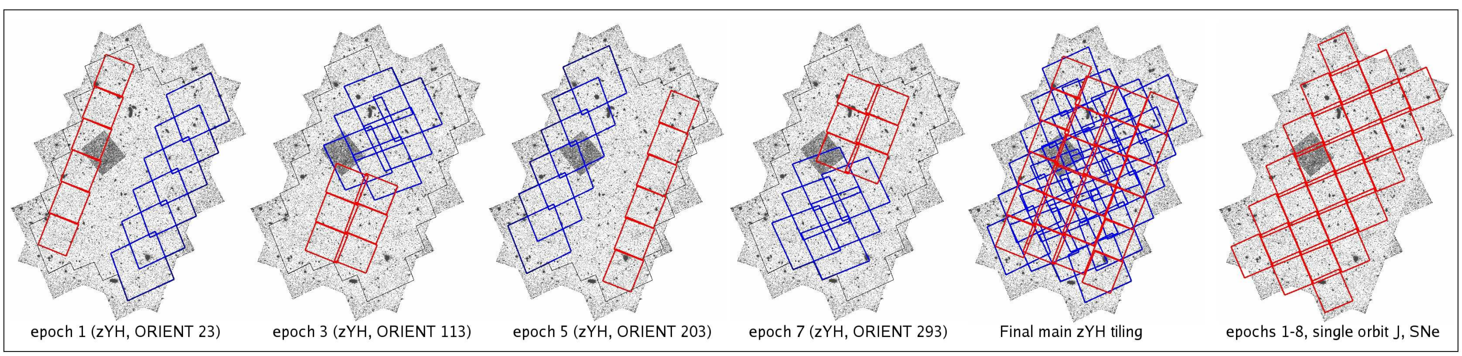

Figure 10: Tiling/visit strategy for GOODS-S (and by analogy, GOODS-N). Four "deep" epochs (1-3-5-7) spaced by 90 days image in Y/H so that ACS z_{850} parallels land within the GOODS field;

WFC3/IR footprint is in red, ACS in blue, and final coverage in light black outline; approximate ORIENTs are in parentheses. Final panel illustrates a single-orbit WFC3 J-band "shallow" tiling every 45 days (epochs 1-8) for the rolling SNe search, ultimately coadded with the main tiling. Even-numbered epochs are tiled as shown, while odd-numbered epochs are tiled in a rectangular pattern similar to the main Y/H observations. ACS parallels are also carried out at 45-day intervals, but are omitted for clarity. The darker shaded area shows the current WFC3/IR image of the UDF (see §6 for issues relating to duplications)..

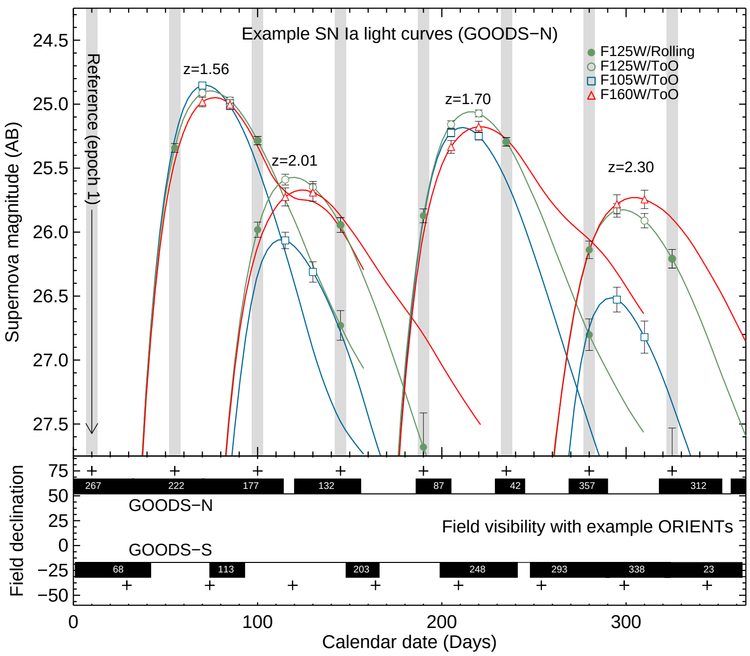

Figure 11: Field visibility, scheduling and sample SN Ia light curves. The lower panel shows the field visibility for GOODS-N and S together with the ORIENTs required. The crosses show the observations separated by 45 days as required by the SN search. The upper panel shows the resulting SN Ia light curves. Four examples are shown over the targeted redshift range. Solid filled circles show data from the rolling search, open points those from ToO observations (§4).

Description of the Observations

Our observing strategy must meet the requirements of all 3 components of our survey. The depth of the WFC3/IR mosaic and the minimum area are set by the first galaxies program, the cadence and details of individual visits are set by the distant SNe search, and the resolution and depth of the final mosaic must permit resolved galaxy studies over a wide range in redshift. A final constraint on the geometrical arrangement of visits is that ACS parallels must add useful optical depth for the first galaxies program.

First Galaxies requirements: WFC3/IR offers a major adance in searching for $z \simeq$7-10 galaxies via improved efficiency and samping and the use of 3 infrared filters (Y_{105}, J_{125} and H_{160}). These ensure significantly reduced foreground contamination and more precise measures of the rest-frame UV continuum slope (Fig. 8, McL09).

The imaging depth is set by the need to probe $\simeq$1 magnitude fainter than $M^\star$ at z=7-8; this addresses the abundance of low luminosity galaxies at early times. The faintest $z = 7$ sources in the WFC3/IR UDF campaign have M_{1500}=-18 ($\simeq$2 magnitudes fainter than $M^\star$) corresponding to 5σ limits of $\simeq$29 (AB) in all 3 bands. Although $M^\star$ is not well-known beyond $z \simeq$6, we estimate that to reach our science goal requires a 5σ detection threshold of Y_{105}=28.0, and to reach the *same* luminosity at $z = 8$ requires a 5σ limit of J_{125}=28.2. Given the in-orbit sensitivity of WFC3/IR with a 0.5-arcsec aperture [McL09], we require 4 orbits in Y_{105}, and 6.5 orbits in J_{125}. The H_{160} depth determined by the need to reliably establish the UV continuum slope, achieved by matching the 3σ depth in H_{160} to the 5σ depth in J_{125}. which requires 4 orbits.

An often-overlooked issue in the effective selection of Lyman-break galaxies is the requirement for the "drop" filter blueward of the detection band. Simulations indicate that the 2σ detection in limit in the "drop" band should be at least 0.8 mag fainter than the 5σ limit in the detection band (not a 1σ limit e.g. adopted by Bou08). For $z \simeq$8 galaxies, this is achieved since our 2-σ limit in Y is $Y_{105} > 29$. However, to fully exploit our new WFC3/IR imaging in the search for $z \simeq$7 galaxies, we require a 2-σ limit of z_{850}>29. This demanding target is unachievable from the ground, and requires $\simeq$ 30 orbits of integration with ACS. Moreover, we also require 2-σ limits at least as deep at all shorter optical wavelengths. The GOODS fields are the only areas with appropriately deep multi-band ACS data from which this essential limit can be met.

Our area requirement is governed by sample statistics and issues relating to cosmic variance. The existing WFC3/IR campaign (GO 11563, PI: Illingworth) will ultimately cover 12.6 arcmin^2 and first estimates (Oe09, Bou09, Bu09, McL09b) suggest it will find 30 z$\simeq$7 galaxies and 12 z$\simeq$8 galaxies. Our proposed program is only 0.7 mag shallower than the current UDF imaging and for the detection/selection of $z \simeq$8 galaxies only 0.35 mag. shallower. But this survey of 200 arcmin^2 would provide an enormous 16-fold increase in area. Our predictions indicate $\simeq$400 $z \simeq$7 galaxies and $\simeq$150 z$\simeq$8 galaxies. For the first time, answers to key questions will not be dominated by cosmic variance uncertainties. Using techniques based on dark matter halo densities discussed in St08, we estimate cosmic variance uncertainties will be reduced from 35% in the Illingworth campaign to <15%.

Distant SNe Ia requirements: Our principal goal is to extend the SNe Ia Hubble diagram to include as many 1.5< z <2.5 events as those already studied in the earlier ACS search over $1 < z < 1.5$ ($\sim$ 15 Kow08; Con09). Estimating the time required is rendered uncertain by a poor understanding of the SN Ia volumetric rate evolution at $z > 1.2$ (Fig. 4). Up to $z \simeq 1$, SDSS+SNLS data (Dild08, Per09) demonstrate a smooth increase in the SN Ia rate with redshift. Beyond $z = 1$, the data are noisy and consistent with a variety of models (Man07; Poz07; Dah08). However, most studies agree upon a rate which correlates with recent star-formation (i.e. stars of age <1Gyr; Man05,06; Sull06; Tot09; Prit09; Per09; Aub09; Schaw09) indicating an abundant population of SNe Ia at $z > 1.5$. Longer delay-times which would imply fewer $z > 1.5$ SNe (e.g. Dahl08) are essentially ruled out by current data. We have fully simulated a SN Ia search with WFC3/IR to select the optimal strategy assuming a variety of rate evolution models, both pessimistic and optmistic. To find 15 $z > 1.5$ SNe Ia requires a search over an effective area of 0.40 deg^2 (a search is defined as two separate visits to the same area).

The most efficient strategy is a 'rolling search', revisiting the same field many times with a cadence shorter than the "rise-time". As demonstrated in SNLS (Sull07), such a strategy locates useful SNe Ia prior to maximum light (no extrapolation to maximum light brightness), and ensures all images in a given field can be used to locate SNe in real-time (except the very first one which will have no reference image). A SN Ia rest-frame rise-time is $\simeq$17–19 days (e.g., Conl06), therefore allowing for time dilation the cadence of the search must be no more than $\sim$45 days. The detailed strategy is a trade-off between the area imaged at each epoch and the search duration. Simulations indicate the optimum balance is a search on 7 epochs (plus one initial reference), giving a required search area of 0.057 square degrees at each epoch, or about 50 WFC3 pointings (allowing for dithered pointings).

SNe Ia become intrinsically faint below 3000Å and harder to detect when this rest-frame region is redshifted into the observer's frame; above $z = 1.5$, a z_{850} search will be ineffective. This is why a WFC3/IR search is timely and effective (Fig. 4). Simulations show J_{125} is the preferred choice, reaching higher redshifts than Y_{105} and with greater sensitivity than H_{160}. An associated ToO campaign to optimize light curve sampling and provide color information is described in §4.

Emerging Hubble Sequence Requirements: The essential requirements are: sensitivity to $> 10^9\ M_\odot$ galaxies and sub-galactic structures at *rest-frame optical wavelengths* requiring superlative near-IR depth; dithered high-resolution images and a wavelength baseline corresponding to a large rest-frame redshift coverage. The depth requirement for 1 kpc structures sets the number of orbits and the target spatial resolution of 1 kpc can only be achieved by multi-orbit dithered exposures (Fig. 9). Existing ACS images are too shallow for our proposed $z > 1$ measures. Undithered WFC3 images would not have enough resolution to decompose bulges, disks, bars and point source with the required accuracy. Likewise AO images lack the necessary PSF stability and multi-wavelength performance to obtain reliable stellar masses for bulge and disk in the presence of a point source.

The GOODS fields are optimally suited; wider shallower surveys would be severely limited by the undersampled resolution of single-orbit WFC3 observations (Fig. 9); structures in the $10^{11} - 10^9 M_\odot$ mass range do not need large areas to counter cosmic variance. By extending the wavelength baseline of deep $AB \gtrsim 28$ GOODS data from 800 nm to 1600 nm with deep $z'YJH$ imaging we extend the redshift of rest-frame visual data from $z \simeq 0.6$ to $z \simeq 2.2$ while taking maximum advantage of the legacy of multi-wavelength data and ground-based spectroscopy. The addition of deep IR bands to the combination of ACS and IRAC photometry will ensure accurate photometric redshifts *for all galaxy types* out to $z = 3$.

We now turn to requirements common to all three science goals.

Field Selection & Survey Geometry: The 30 orbit depth requirement in ACS z_{850} for reliable selection of z$\simeq$7 galaxies makes our survey uniquely possible in the GOODS fields where there is a considerable legacy of deep HST and Spitzer data. GOODS also provides the required deep ACS imaging shortward of z_{850} over the entire required area, delivering 2-σ detection limits of $B_{435} > 29.4$, $V_{606} > 29.9$, and $i_{775} > 29.3$.

Our proposed strategy is summarized in Fig. 10. Each GOODS field is tiled with a 6×4 WFC3/IR mosaic (24 pointings) observed 8 times in J_{125}. The same fields will also be covered in Y_{105} and H_{160} to a depth of 4 orbits each. Our strategy places $\simeq$ 70% of the ACS parallels within the GOODS fields, yielding 22 orbits of additional z_{850} imaging. Added to the existing 8 orbits of z_{850} imaging satisfies our 30 orbit requirement. This depth of z_{850} imaging is *essential* to exploit the power of WFC3/IR in the search for high redshift galaxies (Fig, 8) and can only be achieved with a multi-epoch strategy in GOODS. Likewise, the total area – 24 pointings – fulfils the area required by the SN search.

Feasibility and Scheduling: The visits in a given GOODS field can be spread over cycles 18-19 or beyond but the 8 epochs for SN searching should always be separated by ~ 45 days. Further, each visit has a limited range of ORIENTs so that a) the tiling strategy in each field can be met, and that b) the essential parallel observations fall into the WFC3/IR fields wherever possible, thereby maintaining an appropriate survey depth in z_{850} band. Using the APT tool, we have assessed the visibility of both fields at our required roll angles (Fig. 10) and have confirmed the feasibility of our strategy.

Total request: Our total allocation for each sub-area is 8 orbits in J_{125}, 4 orbits in Y_{105} and 4 orbits H_{160} – 384 orbits in each GOODS field, or 768 orbits in total. To this we add the 90 orbit ToO requirement discussed in §4. Grand total: 858 orbits. The program could extend over 3 cycles if necessary.

References:

Stark, D. P. et al 2009, in prep. • Stark, D.P. et al 2009 Ap J. 697, 1493 • Bunker, A. et al 2009 astro-ph/0909.2255 • McLure, R. et al 2009 astro-ph/0909.2437 • Oesch, P. et al 2009 astro-ph/0909.1806 • Ouchi, M. et al 2009 astro-ph/0908.3191 • Bouwens, R. et al 2009 astro-ph/0909.1803 • Ouchi, M. et al 2009, in prep • Astier, P. et al 2006 A&A 447, 31 • Riess, A. et al 2004 Ap J 607, 665 • Riess, A. et al 2007 Ap J 659, 98 • Kessler, R. et al 2009 Ap J Supp 185, 32 • Rubin, D. et al 2009 Ap J 695, 391 • Sollerman, J. et al 2009 Ap J 703, 1374 • Mannuci, F. et al 2005 A&A 433, 807 • Sullivan, M. et al 2006 Ap J 648, 868 • Aubourg, et al 2008 A&A 492, 631 • Kowalski, M. et al 2008 Ap J 686, 749 • Copeland, E. et al 2006 Int J Mod Phys 15, 1753 • Dahlen, T. et al 2008 Ap J 681, 462 • Ellis, R.S. et al 2008 Ap J 674, 51 • Somerville, R. et al 2008 MN 391, 481 • Chen, H-W & Marzke, R. et al 2004 Ap J 615, 603 • van Dokkum, P. et al 2008 Ap J 677, L5 • Hopkins, P. et al 2009d astro-ph/0909.2039 • Hopkins, P. et al 2009e astro-ph/0906.5357 • Hopkins, P. et al 2009 MN 398, 898 • Fan, L. et al 2008 ApJ 689, L101 • van der Wel, A. et al 2008 Ap J 688, 48 • Nipoti, C. et al 2009 Ap J 706, L86 • van Dokkum, P. et al 2009 Nature 460, 717 • Cappellari, M. et al 2009 ApJ 703, L34 • Kassin, S.A. 2007 Ap J 660, L35 • Keres, D. et al 2009 MN 395, 160 • Dekel, A. et al 2009 ApJ 703, 785 • Elmegreen, D.M. et al 2009 Ap J 701, 306 • Genzel R. et al 2008 Ap J 687, 59 • Jones, T. et al 2009 astro-ph/0910.4488 • Abraham, R. et al 1999 MN 303, 641 • Abraham, R. et al 1996 MN 279, L47 • Abraham, R. et al 2003 Ap J 588, 218 • Bundy, K. et al 2004 Ap J 601, L123 • Bundy, K. et al 2006 Ap J 651, 120 • Bundy, K. et al 2009 Ap J 697, 1369 • Marchesini, D. et al 2009 Ap J 701, 1765 • Gültekin, K. et al 2009 Ap J 706, 404 • Ota, K. 2008 Ap J 677 12 • Treister, E. et al 2004 Ap J 616, 123 • Jahnke, K. et al 2009 astro-ph/0907.5199 • Merloni et al 2009 astro-ph/0910.4970 • Bouwens, R. et al 2008 Ap J 686, 230 • Conley, A. et al 2006 Ap J 644, 1 • Dilday, B. et al 2008 Ap J 682, 262 • MacArthur, L. et al 2008 Ap J 680, 70 • MacArthur, L. et al 2009 submitted • Richard, J. et al 2008 Ap J 685, 705 • Bunker, A. et al 2004 MN 355, 374 • Conley, A. et al 2009, in prep. • Perrett et al 2009, in prep. • Mannucci, F. et al 2007 MN 377, 1229 • Poznanski, D. et al 2007 MN 382, 1169 • Totani, T. et al 2008 PASJ 60, 1327 • Pritchet, C. et al 2008 ApJL 683, 25 • Schawinski, K. 2009 MN 397, 717 • Bluck, A et al 2009 MNRAS 394, L51 • Benson et al. 2007, MNRAS, 379, 841 • Cassata et al. 2009, astro-ph/0911.1158 • Conselice, C. et al 2008 MNRAS 386, 909 • Genel, S. et al 2008 ApJ 688, 789 • Lotz, J. et al 2008 ApJ 672, 177 • McGill et al. 2008, ApJ, 673, 703 • Ferrarese, L. & Ford, H. 2005, SSRv, 116, 523 • Peng, C. et al 2006, ApJ, 649, 616 • Bennert, V.N. et al 2009, ApJ, submitted • Greene & Ho, L. 2007, ApJ, 667, 131 • Treu, T. et al 2007, ApJ, 667, 117 • Sarajedini, V. et al. 2006, ApJS, 166, 69 • Nugent, P. et al 2006 Ap J 645, 841

• Zabetti et al 2009 • Abraham, R. et al 2007 • Nair & Abraham, R. 2009 • Elvis, M. et al 1994 • Quimby, R. et al 2009 • Cooke, J. et al 2009

Special Requirements

ToO Requirements: We will follow up our SNe Ia with additional observations to fully determine their properties and photometric characteristics in order to construct a Hubble diagram. $z > 1.5$ SNe Ia must be screened from lower-z interlopers of other types in near real-time and ultimately a spectroscopic redshift must be secured. Based on successful ground-based SN Ia surveys (Ast et al. 06; Kess et al. 09), SNe must be photometrically monitored in the rest-frame every 5–7 days to +20–+30 after maximum light for a robust measure of the SN light curve shape, The SNe require observations in 3 filters sampling the rest-frame range 3500–7000Åensuring two independent colors and an accurate color correction.

Our screening will use a combination of existing GOODS galaxy photometric and spectroscopic data, and, where available, color selection from our parallel z_{850} data (we estimate ~60% of our SNe will have z_{850} data at the time of detection). A single color can effectively discriminate SN types in a rolling search especially when a redshift estimate is available (e.g., Rie04; Sull06). Spectroscopy will be challenging for these targets but conducted with 8-10m spectrographs in conjunction with the planned deep spectroscopic surveys (§1.2).

Although data at $\lambda < 3500$ has been successfully used for color measurements in the SNLS (e.g. Con08), its use is both harder to calibrate and k-correct, and the effect of dust is more pronounced. At $z > 1.5$, the SN light curves must primarily be constrained by the 3 WFC3/IR filters. As it is too expensive to observe the entire GOODS fields in all 3 filters for all 8 epochs, we propose standard ToO observations to build the light curves in Y and H. Fig. 10 shows examples of light curves obtainable via this strategy.

Each SN would be observed on two intermediate epochs between the main 45 day rolling search (i.e., at 15 and 30 days after detection). At z=1.5 (2.0), in the rest-frame these will be a6 (4.5) and 12 (9) days after maximum light. Observations in Y_{105}, J_{125}, and H_{160} are required for both epochs; a further J_{125} epoch at 45 days from the rolling search completes the light curve. Thus each SN requires 6 additional ToO orbits or 90 orbits for 15 SNe.

Coordinated parallels: We require ACS z_{850} observations concurrent with the repeated WFC3/IR tiling of our survey area (§3, Fig. 9).

CVZ observations: Although GOODS-N is in the CVZ viewing zone, we assumed standard orbit durations following advice from STScI given our restricted ORIENTs (Fig. 10). Should longer visits be possible we would schedule multi-filter WFC3/IR observations at each visit. This will improve light curve data for SNe and the depth of high z galaxy data.

Coordinated Observations

None.

Justify Duplications

The proposed WFC3/IR images must be substantially deeper and in more filters than the extant NICMOS data. Combining WFC3 and NICMOS data is not desirable given the different point spread functions. The proposed parallel ACS z_{850} observations are required to increased the depth of the GOODS ACS images (Fig. 8). Illingworth (GO 11563) has observed the UDF (within GOODS-S, Fig. 10) in our proposed WFC3/IR filters. However, even if we forego repeated visits to this small sub-area (reducing our supernova search area by 1 part in 48), we would reduce the depth of parallel ACS z_{850} imaging in 3 areas around the field reducing by 1/16th the area searched for $z > 7$ galaxies. Accordingly, we propose to revisit this field to maximize the delivery of both high z galaxies and distant SNe.

Management Plan

The Team: The PI has assembled a focused team with strong Co-I's which have worked together on relevant HST datasets for over a decade. The time-critical SN campaign will pace the data reduction and science products. The team has valuable experience in the timely processing and analysis of HST and SNe datasets. Members were the first to publish science results from the early WFPC-2 HDF and ACS UDF exposures (Ab96, Bu04) and amongst the first for the recent WFC3/IR release (Bu09, McL09b). The team has effectively exploited the GOODS archive; the PI alone has published 28 papers based on this dataset.

Personnel: The team comprises 3 sub-groups with science leaders - first galaxies (Dunlop), distant SNe (Sullivan), emerging Hubble sequence (Treu). Each has access to a large team of students and postdocs. The international nature of the team (Canada, UK, Japan, Australia) ensures additional funding from non-NASA sources for postdoctoral support and access to non-US ground-based facilities.

Ellis is an established observational leader who has energetically pursued HST and ground-based surveys of SNe and faint galaxies near and far. Dunlop & Bunker have led in the search for distant galaxies. Input on models of reionization is provided by Loeb and Nagamine. Ouchi, Iye and Shimasaku lead in exploitation of faint Subaru data. Sullivan played a key role in the success of the SNLS survey; his unique experience has been critical in shaping the SN component. Treu and Glazebrook have led many analyses of galaxy evolution over $0 < z < 2$. With modeling from P. Hopkins and Brooks, the team has balanced skills over a wide range of topics while remaining refreshingly focused.

Data processing & timeline for public data releases: Individual epochs will be processed in real time at the National Energy Research Computing Center (NERSC) so that transients can be triggered immediately for ToO campaigns (led by Nugent). Our team has demonstrated its ability to successfully operate in this mode via the successful STIS campaign of nearby events (GO 11721, PI: Ellis). NERSC houses on spinning disk the Palomar Transient Factory archive of images and subtractions from its rolling search. Over 50GB of PTF data are processed nightly, subtracted from references and transients announced <12 hrs. With this experience we plan to release single epoch data and all transient detections 24 hours after they are made available by STScI.

A Caltech/UCB team will produce a continuously updated stacked mosaic and catalog of ever-deeper ACS/WFC3-IR photometry. Catalogs will be merged with other datasets (ACS GOODS, Subaru/VLT K, IRAC & Chandra). Intermediate catalogs will be publicly available 1 month after each visit. Each year-end, the ACS/WFC3-IR data will be reprocessed to take advantage of improved registration, defect removal and new calibrations. In consultation with our consultant Koekemoer (STScI), who designed MultiDrizzle and has much expertise with large HST imaging surveys, we will investigate new instrumental effects and develop/deliver new software as necessary. An optimally-reduced dataset will be the main legacy into the JWST era. Final mosaics with noise maps and multi-wavelength catalogs will be released within 12 months of completion of each GOODS field.

Dissemination of public data products: Access to data products will be made available through an agreement with the Canadian Astronomical Data Centre (CADC) operated by the Herzberg Institute of Astrophysics, Victoria, B.C. CADC is a recognized world leader in data archiving and manages numerous archives (e.g CFHT, JCMT, Gemini and FUSE, as well as advanced HST data products and a mirror of the HST archive).

The CADC has committed to providing access to data products at both a low-level (raw data) and a high-level (reduced data, catalogs) along with data browsing tools. The model will be based on that for the CHFT Legacy Survey. CADC will provide: i) personnel to implement the database and data dissemination portal. ii) data hosting of both raw and reduced images, and of multiple versions of catalogs. iii) tools for catalog browsing. iv) graphical tools for image browsing and subset selection (i.e. creation of postage stamps). v) technical assistance to team members on matters relating to data archiving.

Past HST Usage and Current Commitments

The PI has led the following relevant HST programs in the last 5 years:

GO 11721: Verifying the Utility of Type Ia Supernovae as Cosmological Probes: Evolution & Dispersion in the Ultraviolet Spectra: Standard ToO STIS spectra are being taken for 35 nearby SNe Ia to understand the dispersion and possible evolution in their UV spectra. The program successfully demonstrates the feasibility of a targeted ToO campaign of the kind proposed in §4.

GO 10504: Characterizing the Sources Responsible for Cosmic Reionization: Using massive clusters 12 gravitationally-lensed systems were identified of which 5 were considered promising z≃7 sources (Ric09). An unlensed depth fainter than in the NICMOS/ACS UDF was obtained. The program demonstrated a likely steep faint end slope for the $z \simeq 7$ LF, as now suggested by the first WFC3/IR results (Fig. 1).

AR 10293 : The Assembly History of Disks & Bulges out to z=1: Spirals to z≃1 were analyzed in both GOODS fields with Keck spectra to construct the evolving Fundamental Plane for spiral bulges (MacA08,09). The program demonstrated the utility of resolved galaxy studies and the synergy with Keck spectroscopy.

HST publications from the PI over the last 5 years: Out of 102 refereed papers published by the PI during this period, 51 involved analyses of HST data. Already a third have >75 citations each. A selected list is available on